Surface Plasmon Polaritons Excitation at the Interface of Graphene and Sodium Media

Jehan *Akbar*[1,2,3], Xu *Bin*[1], Lianping *Hou*[4], John H *Marsh*[4], Xuefeng *Liu*[1]
[1]*School of Electronic and Optical Engineering, Nanjing University of Science and Technology,200 Xiaolingwei, Nanjing, 210094 China,*
[2]*Department of Physics, Hazara University Mansehra KPK, Pakistan,*
[3]*Abdus Salam International center for Theoretical Physics, Trieste, Italy,*
[4]*James Watt School of Engineering, University of Glasgow,G12 8QQ, UK, and*
*(The first and second author have equal contribution)**

The surface plasmon polaritons (SPPs) are excited at the interface of Sodium and Graphene media due to the effective control of dielectric functions of the two media. The absorption and dispersion behaviors of SPPs waves are modified with changing the strength of control fields and their phases. The normal and anomalous SPPs dispersion are controlled for slow and fast SPPs propagation. The group index changes in the range $-2000 \leq n_g \leq 2000$ with the strength of control frequencies. The maximum SPPs group velocity is measured to be $1.5 \times 10^5 m/s$ and the maximum propagation length is measured to be 80λ. Furthermore, the propagation length of SPPs can be controlled with strength of the control fields and their phases variation. These controlled SPPs have potential applications in optical tweezers, nano-photonics, plasmonster technology and sensing technology.

I. INTRODUCTION

Plasmonics is a rapidly growing field that appeared in early 1950's with the discovery of SPPs. Plasmonics very quickly expanded from physics to engineering, medicine, biology and the environmental sciences [1–3]. In the last decade, there have been a significant growth in plasmonics and its applications in the field of spectroscopy and sensing technology[4] optical tweezers[5, 6] nano-photonics[7] and radiations guiding[8]. Recently, huge progress has been made and researchers are attracted towards the emerging and potentially important field of plasmonics. Basically, plasmonics deals with the study and investigations of interaction between light and electrons (conduction electrons) in a metal. Under certain conditions, the photons and electrons are coupled together to form a hybrid of photon and exited electronic level, which produces an enhanced optical near-field at the metallic interface or inside the metallic nano-structures. The energy of surface plasmons (SPs) is very important and it depends on the competing forces which are involved in the phenomenon such as excitation, and nucleus-electrons interactions. The resonance energy strongly depends on the material composition, number of structures and the shape. Interaction of photons with free electrons on metal surface form propagating excitation waves which generates SPPs. These electromagnetic (EM) excitations propagates like a wave along the metal-dielectric interface and their amplitude exponentially decays with increasing the distance from interface. Therefore, the SPPs are surface EM waves, with confined EM-field in the vicinity of metal-dielectric interface. There is an enhancement of the electromagnetic field at the interface due to this confinement, which leads to an extra-ordinary sensitivity of SPPs to the surface conditions and this could be utilized for studying, surface roughness, adsorbates on the surface and other related phenomenon. By altering the structure of metal surface, properties of SPs, particularly their interaction with light can be tailored, which can lead to development of new types of photonic devices. The excitation of SPPs can overcome the fundamental diffraction limit to about one half or the optical wavelength and offer advantages to be used for light manipulation at sub-wavelength scale. The control and manipulation of light using SPPs offer significant advantages and overcome many challenges in nano photonic devices such as low performance, low stability and low efficiency. A lot of research has been dedicated to SPPs of metals such as Gold and Silver but due to high coherence, the applications of metal SPPs are limited to optical processing devices. The nano-structures fabricated using multiple materials (multi-layered metal structures separated by dielectrics, dielectric coated with metals, semiconductors coated with metals etc) have been used to tailor the plasmonic characteristics of substrates for increasing the local E-field strengths or adding new functionalities. Due to the excellent electrical and optical properties and strong confinement because of two dimensional nature, Graphene plasmonics have attracted researchers[10]. Graphene plasmonics is an ideal candidate for future applications due to its lower losses and efficient localization of waves (ultra-compact mode confinement)

*Electronic address: jehan@hu.edu.pk

in THz and infrared frequency range[11]. Another major advantage of Graphene is its tunability of SPPs as the doping and electrical gating can easily control its carrier densities. Significant achievements in Graphene plasmonics have been made both theoretically and experimentally[12]. Bakhtawar et al investigated the control and modification of SPPs generated at the interface of a dielectric and Graphene medium under the effect of Kerr non linearity[13]. However to realise reliable and efficient plasmonic based quantum devices, a lot of research still need to be done to explore and understand excitation, propagation, and detection of SPPs in Graphene, similar to those in metals.

Upto the best of our knowledge there are no reports on the study of excitation of SPPs and its decay at the interface of Sodium and Graphene. In this work, we present SPPs excitation and decay at the interface of Sodium and Graphene for advanced plasmonster and sensor technology. We have investigated the effects of Rabi frequencies and probe detuning and their phases on the decay, dispersion, sub-luminal and super-luminal propagation and propagation length of SPPs.

II. MODEL OF THE ATOMIC SYSTEM

The four level atomic configurations of a Sodium D_1 line and Graphene medium are shown in Fig.1. Inside the figure, four level Sodium atomic configuration is shown above and Graphene configuration is shown below on Graphene structure. For Sodium medium, the probe field E_{ps} which has Rabi frequency Ω_{ps} is coupled between states $|a\rangle$ and $|d\rangle$. The states $|a\rangle$ and $|c\rangle$ are coupled with a control field E_3 having Rabi frequency Ω_3. The $|a\rangle$ and $|b\rangle$ are coupled with control field E_4 having Rabi frequency Ω_4. The states $|b\rangle$ and $|c\rangle$ are coupled with a control field E_5 having Rabbi frequency Ω_5. The detuning of these fields are Δ_{ps} and $\Delta_{3,4,5}$ respectively. The decay rates between these states are $\Gamma_{da,dc,cb,ba}$.

For the four level Graphene configuration, the probe field E_{pg} which has Rabi frequency Ω_{pg} is coupled between states $|1\rangle$ and $|4\rangle$. The two control fields $E_{1,2}$ having Rabi frequencies $\Omega_{1,2}$ are coupled to states $|2\rangle \Leftrightarrow |3\rangle$ and $|3\rangle \Leftrightarrow |4\rangle$.

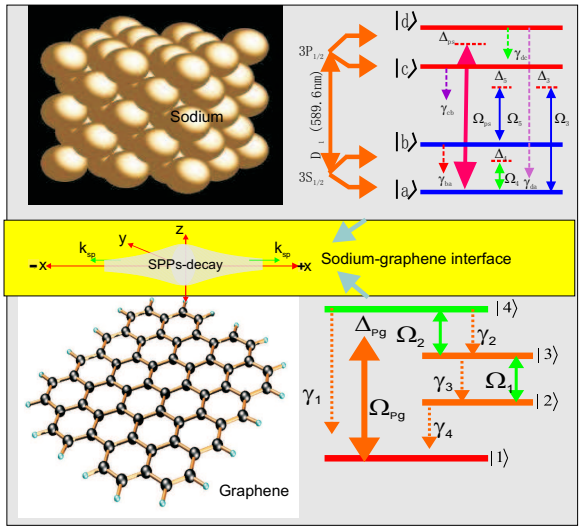

FIG. 1: Schematic showing energy diagrams of both four level atomic systems and their interface

The Hamiltonian in the interaction picture for Sodium medium of four level atomic system can be written as

$$\begin{aligned} H_{ps}^{(I)} &= -\frac{\hbar}{2}\Omega_{ps}e^{-i\Delta_{ps}t}\,|a\rangle\langle d| - \frac{\hbar}{2}\Omega_3 e^{-i\Delta_3 t}\,|a\rangle\langle c| \\ &\quad -\frac{\hbar}{2}\Omega_4 e^{-i\Delta_4 t}\,|a\rangle\langle b| + \frac{\hbar}{2}\Omega_5 e^{-i\Delta_5 t}\,|b\rangle\langle c| + H.C \end{aligned} \tag{1}$$

Where H.C represent the complex conjugate part of the hamiltonian, $\hbar$ is the plank constant, Ω_{ps} is the frequency associated with the probe field and Δ_{ps} is the detuning of the probe field in sodium atomic system. Similarly, the

Hamiltonian in the interaction picture for Graphene medium can be written as:

$$H_{pg}^{(I)} = -\frac{\hbar}{2}\Omega_1 e^{-i\Delta_1 t}\left|2\right\rangle\left\langle 3\right| - \frac{\hbar}{2}\Omega_{pg} e^{-i\Delta_{pg} t}\left|1\right\rangle\left\langle 4\right| - \frac{\hbar}{2}\Omega_2 e^{-i\Delta_2 t}\left|3\right\rangle\left\langle 4\right| + H.C \tag{2}$$

Where Ω_{pg} is the frequency of the probe field and Δ_{pg} is the detuning of the probe field in the Graphene atomic system. The detunings of these fields are related to their corresponding angular frequencies and atomic states resonance frequencies as: $\Delta_1 = \omega_{23} - \omega_1$, $\Delta_2 = \omega_{34} - \omega_2$, $\Delta_{pg} = \omega_{14} - \omega_p$. The decay rates are $\gamma_{1,2,3,4}$. The master equation for density matrix is given as:

$$\dot{\rho} = -\frac{i}{\hbar}[\rho, H_{pg,pd}^{(I)}] - \frac{1}{2}\sum \Gamma_{ij}(\sigma^\dagger\sigma\rho + \rho\sigma^\dagger\sigma - 2\sigma\rho\sigma^\dagger) \tag{3}$$

where $\sigma^\dagger$ is raising operator and σ is lowering operator for the atomic decays.

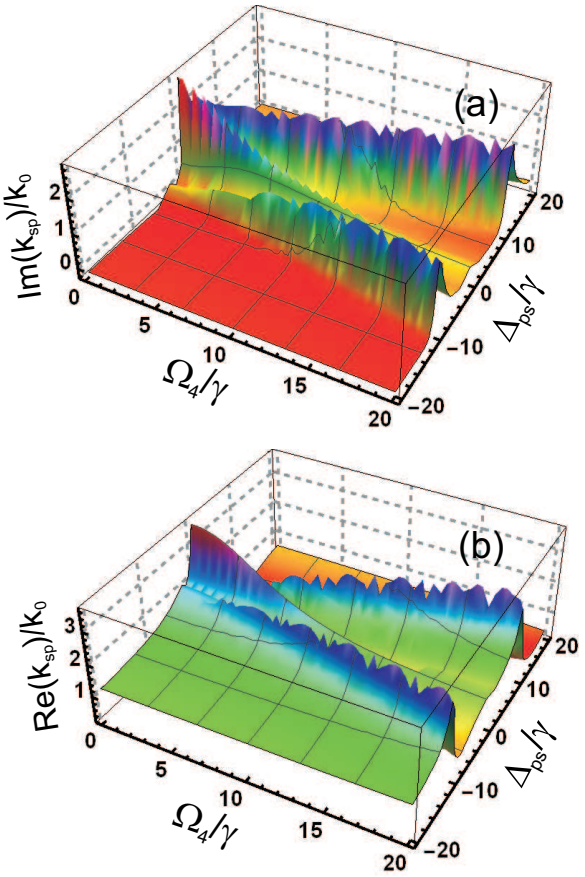

FIG. 2: Dispersion relation of surface plasmon. Plot (a) shows the imaginary part of k_{sp} and plot (b) shows the real part of k_{sp} such that $\gamma_{1,2,3,4} = 2\gamma$, $\Gamma_{da,cb,ba,dc} = 2\gamma$, $\Delta_{1,2,3,4,pg} = 0\gamma$, $|\Omega_{1,2}| = 2\gamma$, $|\Omega_3| = 3\gamma$, $|\Omega_5| = 5\gamma$

Both the systems are solved for explicitly time independent density matrix equations using master Eq.3. Further sixteen density matrix equations are solved for each of the two systems. The coupled rate equations are chosen from the sixteen density matrix in explicitly time independent form. For Graphene medium, we used first order perturbation and initial population conditions $\widetilde{\rho}_{11}^{(0)} = 1$ and $\widetilde{\rho}_{44}^{(0)} = \widetilde{\rho}_{ij}^{(0)} = 0$. The following expression is used to obtain the solution of $\widetilde{\rho}_{ad}^{(1)}$ and $\widetilde{\rho}_{14}^{(1)}$ for gain assisted and Graphene system.

$$Z(t) = \int_{-\infty}^{t} e^{-A(t-t')} B dt' = A^{-1}B, \tag{4}$$

where $Z(t)$ and B are column matrices while A is a $n \times n$ matrix. The calculated $\widetilde{\rho}_{ad}^{(1)}$ for Sodium atomic system is:

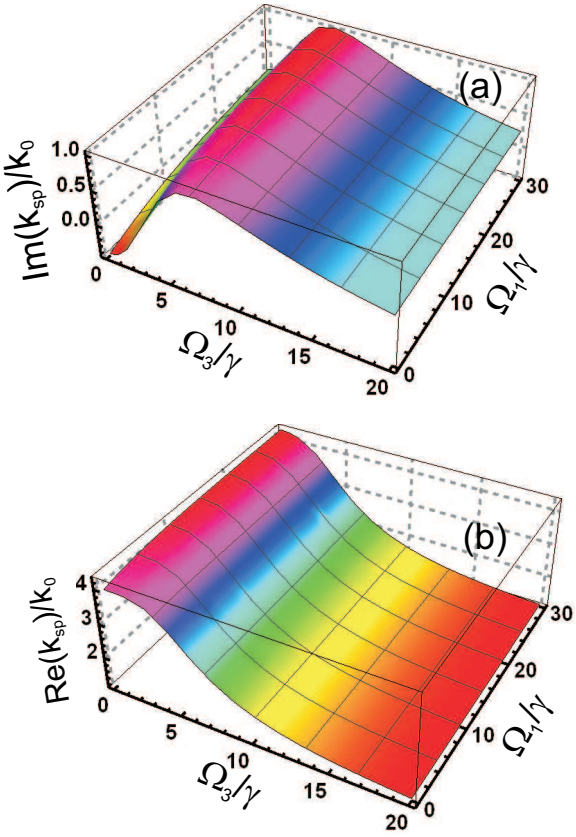

FIG. 3: Dispersion relation of surface plasmon. Plot (a) shows the imaginary part of k_{sp} and plot (b) shows the real part of k_{sp} such that $\gamma_{1,2,3,4} = 2\gamma$, $\Gamma_{da,cb,ba,dc} = 2\gamma$, $\Delta_{1,2,3,4,pg,ps} = 0\gamma$, $|\Omega_{2,4}| = 2\gamma$, $|\Omega_5| = 5\gamma$

$$\overset{\sim}{\rho}{}^{(1)}_{ad} = -\frac{(4A_1A_2A_3 + \Omega_5^2)}{Q - 2i(4A_1A_2A_3 + A_2\Omega_3^2 + A_3\Omega_4^2 + A_2\Omega_5^2)} \tag{5}$$

The calculated susceptibility for the Sodium atomic system obtained from density matrix element $\widetilde{\rho}^{(1)}_{ad}$ is:

$$\chi_s^{(1)} = \frac{2N|\varrho_{ad}^2|}{\epsilon_0\hbar\Omega_{pd}}\widetilde{\rho}^{(1)}_{ad} \tag{6}$$

Also the first order density matrix for the Graphene medium is calculated as:

$$\overset{\sim}{\rho}{}^{(1)}_{14} = \frac{i[\Omega_p B_1 B_2 + \frac{1}{4}|\Omega_1|\Omega_2|e^{i(\varphi_1-\varphi_2)}]}{2(B_1B_2B_3 + \frac{1}{4}|\Omega_1|\Omega_2|e^{i(\varphi_1-\varphi_2)} + \frac{B_1|\Omega_2|^2}{4})} \tag{7}$$

The susceptibility for Graphene is:

$$\chi_g^{(1)} = \frac{2N\varrho_{14}^2}{\epsilon_0\hbar\Omega_{pg}}\overset{\sim}{\rho}{}^{(1)}_{14} \tag{8}$$

where N= 5×10^{12} atoms per cm^3 is the density of four-level atoms and $\varrho_{14,ad}$ are the atomic dipole moments.

$$A_1 = i\Delta_{ps} - \frac{1}{2}(\Gamma_{da} + \Gamma_{ba}) \tag{9}$$

$$A_2 = i(\Delta_{ps} - \Delta_4) + \frac{1}{2}\Gamma_{cb} \tag{10}$$

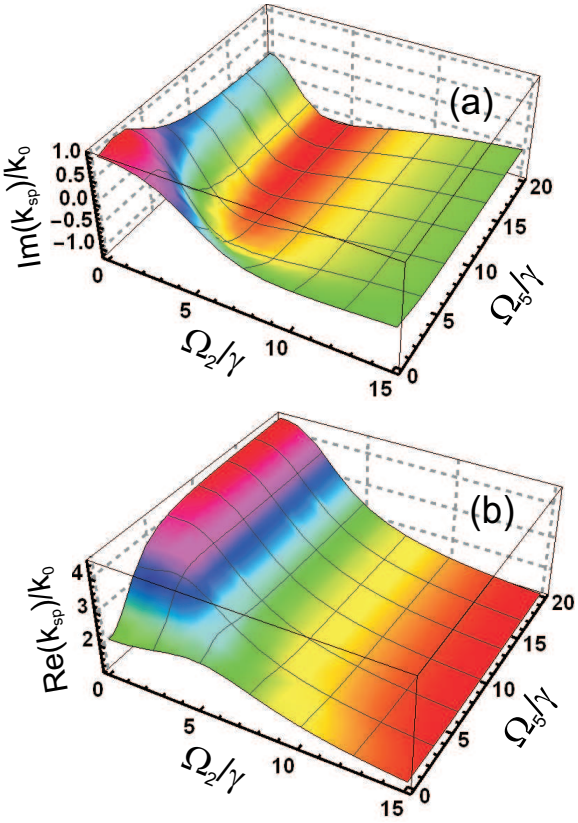

FIG. 4: Dispersion relation of surface plasmon. Plot (a) shows the imaginary part of k_{sp} and plot (b) shows the real part of k_{sp} such that $\gamma_{1,2,3,4} = 2\gamma$, $\Gamma_{da,cb,ba,dc} = 2\gamma$, $\Delta_{1,2,3,4,pg,ps} = 0\gamma$, $|\Omega_{1,3,4}| = 2\gamma$

$$A_3 \;=\; i(\Delta_{ps} - \Delta_3) + \frac{1}{2}\Gamma_{dc} \tag{11}$$

$$B_1 \;=\; i(\Delta_{pg} - \Delta_2 - \Delta_1) + \frac{1}{2}(\gamma_1 + \gamma_4) \tag{12}$$

$$B_2 \;=\; i(\Delta_{pg} - \Delta_2)\frac{1}{2}(\gamma_1 + \gamma_2 + \gamma_4) \tag{13}$$

$$B_3 \;=\; i\Delta_{pg} + \frac{1}{2}(\gamma_1 + \gamma_4) \tag{14}$$

$$Q \;= \Omega_3\Omega_4\Omega_5(\exp(i\varphi) + \exp(-i\varphi)) \tag{15}$$

The dispersion relation for SPPs is:

$$k_{sp} = \sqrt{\frac{(1 + 4\pi\chi_s^{(1)})(1 + 4\pi\chi_g^{(1)})}{2 + 4\pi(\chi_s^{(1)} + \chi_g^{(1)})}} \tag{16}$$

where $k_{sp} = k_0 n_{sp}$. The phase velocity of plasmon polaritons can be written as $v_p = c/n_r^{sp}$. The intensity of SPPs decreases exponentially along the interface of Sodium and Graphene media according to $e^{-2k_{sp}L_x}$, where L_x

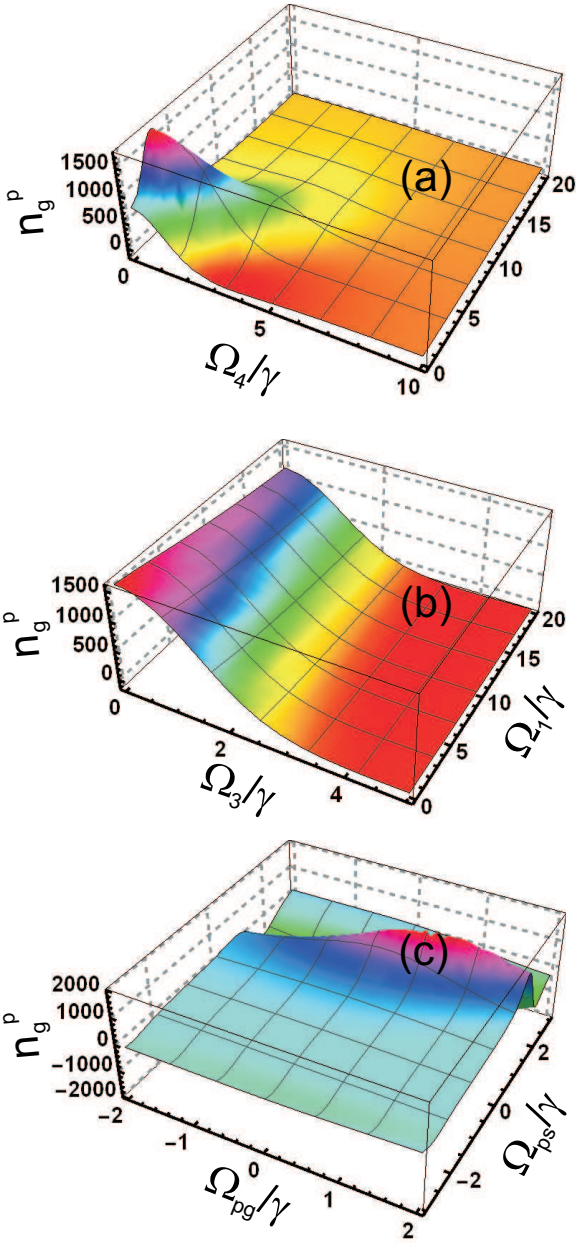

FIG. 5: Group index of SPPs such that $\gamma_{1,2,3,4} = 2\gamma$, $\Gamma_{da,cb,ba,dc} = 2\gamma$, $\Delta_{1,2,3,4,pg,ps} = 0\gamma$, (a) $|\Omega_{1,3,5}| = 2\gamma$ (b) $|\Omega_{2,4,5}| = 2\gamma$ (c) $|\Omega_{1,2,3,4,5}| = 2\gamma$

is the propagation length. The propagation length of SPPs is related to imaginary part of k_{sp} and is written as $L_x = 1/2Im(k_{sp})$. The group index of SPPs can be written as:

$$n_g^{sp} = \frac{1}{k_0}\sqrt{\frac{(1+4\pi\chi_s^{(1)})(1+4\pi\chi_g^{(1)})}{2+4\pi(\chi_s^{(1)}+\chi_g^{(1)})}} + \frac{\omega}{k_0}[\frac{\partial}{\Delta_{pg}}\sqrt{\frac{(1+4\pi\chi_s^{(1)})(1+4\pi\chi_g^{(1)})}{2+4\pi(\chi_s^{(1)}+\chi_g^{(1)})}} + \frac{\partial}{\Delta_{ps}}\sqrt{\frac{(1+4\pi\chi_s^{(1)})(1+4\pi\chi_g^{(1)})}{2+4\pi(\chi_s^{(1)}+\chi_g^{(1)})}}] \quad (17)$$

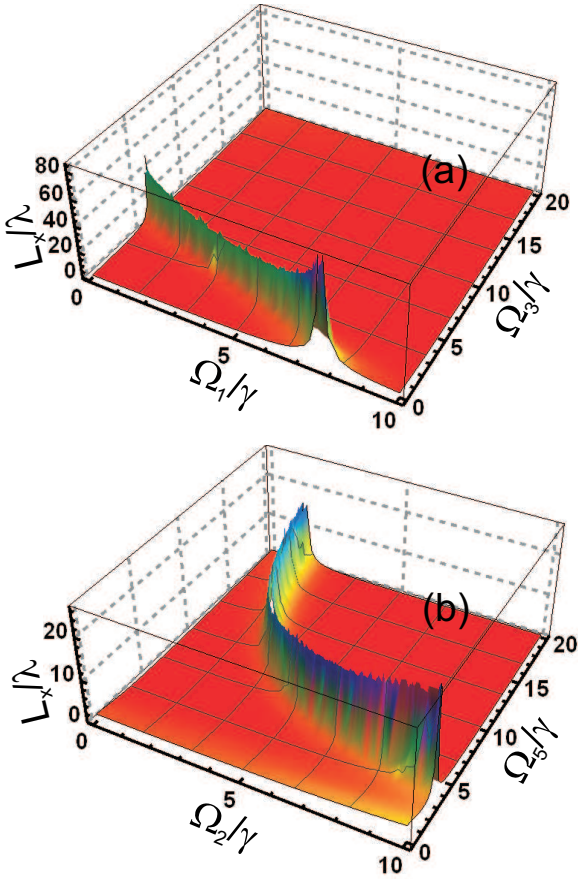

FIG. 6: Propagation length of SPPs such that $\gamma_{1,2,3,4} = 2\gamma$, $\Gamma_{da,cb,ba,dc} = 2\gamma$, $\Delta_{1,2,3,4,pg,ps} = 0\gamma$, (a)$|\Omega_{2,4,5}| = 2\gamma$ (b) $|\Omega_{1,3,4}| = 2\gamma$

III. RESULTS AND DISCUSSION

The results are presented for real and imaginary parts of dispersion relation (k_{sp}) of SPPs. The real part of k_{sp} is related to the dispersion and imaginary part is related to the damping spectra of SPPs. If $Re(k_{sp}) > k_0$, the SPPs propagate along the interface and if $Re(k_{sp}) < k_0$, the SPPs can not propagate along the interface of two media and die out with time. We have, $k_0 = 2\pi/\lambda$ is the free space wave-vector of EM-waves and λ is its wavelength. The decay rate γ is taken as a comparison unit for other parameters, its value is taken as $10MHz$ and the other parameters are scaled to this decay rate γ. The values of parameters $\hbar, \mu_0, \epsilon_0 = 1$ are taken in atomic units and $\varphi_{1,2} = \pi/6, \pi/4$, while $\varphi = \pi/2$.

The Fig.2 shows the real and imaginary parts of dispersion relation (k_{sp}) of SPPs vs. control fields Rabi frequencies of $\Omega_{2,4}$. The imaginary part of k_{sp} shows damping spectrum and the real part shows dispersion spectrum of SPPs waves. The damping value is maximum at $\Omega_4 = 0\gamma$ with a single sharp peak. In the presence of control field, the single sharp peak splits into a doublet with its width increasing with the value of control field Ω_4/γ as shown in FIG.2a. The real part of k_{sp} is greater than the free space EM wave-vector (k_o) which means that SPPs waves are propagating at interface of the two media. In larger interaction region, there is more damping which leads to larger value of dispersion as shown in the FIG.2b.

The Fig.3 presents the plots for real and imaginary parts of k_{sp} with control fields Rabi frequencies $\Omega_{1,3}$, while keeping the values of phases of the control fields constant. The damping of SPPs waves initially increases with increase in the control field frequency Ω_3 till $\Omega_3 = 5\gamma$ and then monotonically decreases with further increase in the value of Ω_3. Furthermore, the damping does not depend on the Rabi frequency Ω_1 as shown in FIG.3a. The FIG.3b shows that the slope of dispersion of SPPs is anomalous with Ω_3 and unaffected with Ω_1.

Similarly, FIG.4 shows the real and imaginary part of (k_{sp}) dispersion relation of SPPs vs control fields Rabbi frequencies of $\Omega_{2,5}$. As shown in the Fig, the damping of SPPs decreases with increasing the value of Ω_2 and comparatively decreases slowly with increasing the value of Ω_5. The dispersion slope of SPPs is anomalous with

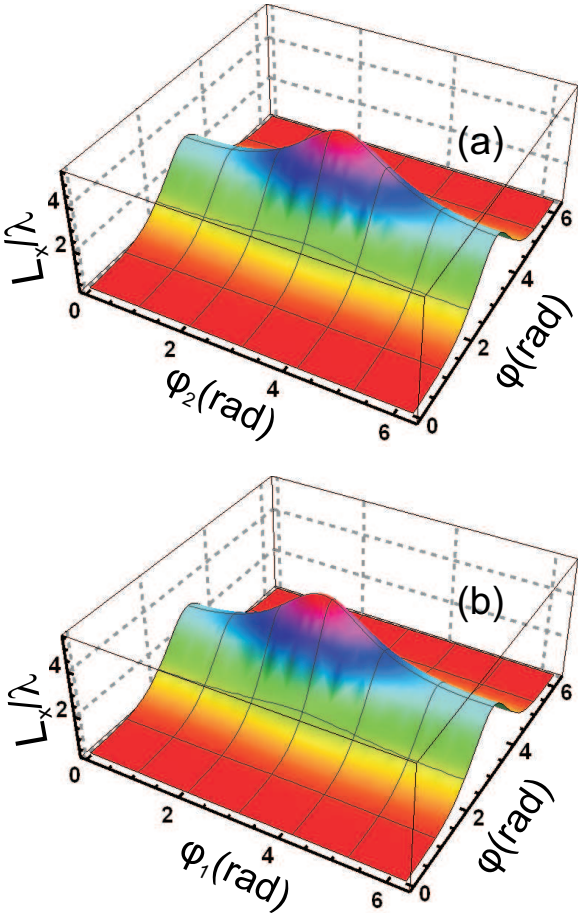

FIG. 7: Propagation length of SPPs such that $\gamma_{1,2,3,4} = 2\gamma$, $\Gamma_{da,cb,ba,dc} = 2\gamma$, $\Delta_{1,2,3,4,pg,ps} = 0\gamma$, $|\Omega_{1,2,3,4,5}| = 2\gamma$ (a)$\varphi_2 = 0$ (b) $\varphi_1 = 0$

the control field Rabi frequency Ω_2 and normal with Ω_5. This shows sub-luminal (increasing Ω_5)and super-luminal (increasing Ω_2) propagation of SPPs depending on the control fields Ω_2 and Ω_5 as shown in FIG.4b

FIG.5 shows the group index of SPPs vs control fields Rabi frequencies $\Omega_{2,4}$, $\Omega_{1,3}$ and detuning of probe fields. FIG.5a shows that in the absence of control fields i.e. $\Omega_{2,4} = 0\gamma$, maximum value of group index (1500) is obtained. As the value of Rabi frequencies of control field increases, the group index decreases which leads to increase in velocity of SPPs. The dependence of group index on the values of $\Omega_{1,3}$ is presented in FIG.5b. It is clear from the figure that the group index is rapidly decreasing with increase in Ω_3 while gradually decreasing with increase in Ω_1. The dependence of group index of SPPs with respect to probe detuning of Sodium and Graphene is shown in FIG.5c. The figure shows that the group index does not vary with changing the probe detuning of the Graphene while the group index is strongly dependent on the probe detuning of Sodium. This amplies that we can tailor the speed of SPPs with varying the detuning of probe field applied to Sodium.

Fig.6 shows the propagation length of SPPs with control fields Rabi frequencies. The FIG.6a shows variation of propagation length with control fields Rabi frequencies $\Omega_{1,3}$. At $\Omega_1 = 0$, the propagation length exhibits maximum value for a larger value of Ω_3 while as Ω_1 increases the propagation length slowly decreases and shifts towards lower values of Ω_3. After a certain value of Ω_1, the propagation length starts increasing and reaches a maximum value of 80λ for $\Omega_1 = 8\gamma$ as reflected in FIG.6a. The plot shown in FIG.6b shows variation of propagation length with control fields Rabi frequencies $\Omega_{2,5}$. The propagation length increases constantly with increase in Ω_2 and shifts towards lower values of Ω_5 as the value of Ω_2 increases.

Fig.7 shows the propagation length of SPPs at the interface with phases of the control fields. The plot presented in FIG.7a shows variation of propagation length of SPPs with φ_2, φ and FIG.7b show variation of propagation length with φ_1, φ. The propagation length L_x has a maximum value at $\varphi_{1,2} = \pi$ and $\varphi = \pi$ and decreases at other values of phase of the control fields.

IV. CONCLUSIONS

In conclusion, the SPPs waves are excited at the interface of Sodium and Graphene medium due to the effective variation of dielectric functions of the two media. The damping and dispersion behaviors of SPPs are significantly modified with the strength of control fields and their phases. The normal and anomalous slopes of dispersion for SPPs are controlled in the regions of high and low losses regions. In these normal and anomalous slopes of dispersion region, the group velocity substantially become sub-luminal or super-luminal. The normal and anomalous SPPs dispersion are controlled for slow and fast SPPs propagation. The group index varies in the range: $-2000 \leq n_g \leq 2000$ with the strength of control frequencies. Maximum SPPs group velocity is measured to be $1.5 \times 10^5 m/s$. Further, the propagation length of SPPs is controlled with strength of the control fields and their phases variation. The maximum propagation length is measured to be 80λ. The excitation, control and manipulation of SPPs at Sodium-Graphene interface have potential applications in optical tweezers, radiations guiding, nano-photonics, plasmonster technology, sensing technology, data storage devices, solar cell and photovoltaic devices.

[1] Svetlana.V.Boriskina et al. Mat. Today.**16**,375(2013)
[2] N.A.Cinel et al. Opt. Express.**5**,2587(2012)
[3] A.Shalabney, I.Abdulhalim, Laser Photon. Rev.**5**,571(2011)
[4] A.J.Haes et al. MRSBull.**30**,368(2005)
[5] P.J.Reece, Nat.Photon. **2**,333(2008)
[6] M.L.Juan,M.Righini, R.Quidant, Nat.Photon. 5,349(2011)
[7] E.Ozbay, Science **311**,(2006)189
[8] Z.Han, S.I.Bozhevolny, Rep.Prog.Phys. **76**,016402(2013)
[9] A.Vakil, N.Engheta, Science **332**,1291(2011)
[10] Xiao et al. Front. Physics **11**,117801(2016)
[11] Zhefei et al. ACS Photonics **5**,2971(2017)
[12] Zhang et al. Journal of Physics D **45**,1088(2012)
[13] Bakhtawar et al. Chinese Physics B **27**,114215(2018)
[14] K.Kneipp, Phys.Today November,40(2007)
[15] H.J.Xu et al., Appl.Phys.Lett. **100**,243110 (2012)
[16] C. Girard, Rep. Prog. Phys.**68**, 1883 (2005)
[17] J. Mller, B. Rech, J. Springer, M. Vanecek, Solar. Energy. **77**,917(2004)
[18] J. Meier et al.,Sol. Energy Mater. Sol. Cells **74**,457(2002)
[19] S.Zeng et al. chem.Soc.Rev.**43**,3426(2014)
[20] Y.V.Bludov,M.I.Vasilevskiy, N.M.R.Peres, Europhys.Lett. **92**,68001(2010)
[21] M.Crassee Orlita et al., NanoLett. **12**,2470(2012)
[22] K.V.Sreekanth et al., Sci.Rep. 2,737 (2012)
[23] G. S. Agarwal and Shubhrangshu Dasgupta, Phys. Rev. A **70**, 023802 (2004)